

# Synthesis, Characterization, and Cure Chemistry of Renewable Bis(cyanate) Esters Derived from 2-Methoxy-4-Methylphenol

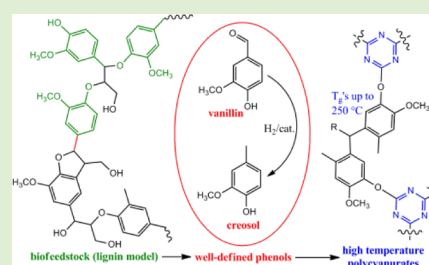
Heather A. Meylemans,<sup>†</sup> Benjamin G. Harvey,<sup>\*,†</sup> Josiah T. Reams,<sup>‡</sup> Andrew J. Guenther,<sup>\*,‡</sup> Lee R. Cambrea,<sup>†</sup> Thomas J. Groshens,<sup>†</sup> Lawrence C. Baldwin,<sup>†</sup> Michael D. Garrison,<sup>†</sup> and Joseph M. Mabry<sup>‡</sup>

<sup>†</sup>Research Department, Chemistry Division, U.S. Navy, NAWCWD, China Lake, California 93555, United States

<sup>‡</sup>Air Force Research Laboratory, Aerospace Systems Directorate, Edwards AFB, California 93524, United States

## S Supporting Information

**ABSTRACT:** A series of renewable bis(cyanate) esters have been prepared from bisphenols synthesized by condensation of 2-methoxy-4-methylphenol (creosol) with formaldehyde, acetaldehyde, and propionaldehyde. The cyanate esters have been fully characterized by infrared spectroscopy, <sup>1</sup>H and <sup>13</sup>C NMR spectroscopy, and single crystal X-ray diffraction. These compounds melt from 88 to 143 °C, while cured resins have glass transition temperatures from 219 to 248 °C, water uptake (96 h, 85 °C immersion) in the range of 2.05–3.21%, and wet glass transition temperatures from 174 to 193 °C. These properties suggest that creosol-derived cyanate esters may be useful for a wide variety of military and commercial applications. The cure chemistry of the cyanate esters has been studied with FTIR spectroscopy and differential scanning calorimetry. The results show that cyanate esters with more sterically demanding bridging groups cure more slowly, but also more completely than those with a bridging methylene group. In addition to the structural differences, the purity of the cyanate esters has a significant effect on both the cure chemistry and final T<sub>g</sub> of the materials. In some cases, post-cure of the resins at 350 °C resulted in significant decomposition and off-gassing, but cure protocols that terminated at 250–300 °C generated void-free resin pucks without degradation. Thermogravimetric analysis revealed that cured resins were stable up to 400 °C and then rapidly degraded. TGA/FTIR and mass spectrometry results showed that the resins decomposed to phenols, isocyanic acid, and secondary decomposition products, including CO<sub>2</sub>. Char yields of cured resins under N<sub>2</sub> ranged from 27 to 35%, while char yields in air ranged from 8 to 11%. These data suggest that resins of this type may potentially be recycled to parent phenols, creosol, and other alkylated creosols by pyrolysis in the presence of excess water vapor. The ability to synthesize these high temperature resins from a phenol (creosol) that can be derived from lignin, coupled with the potential to recycle the composites, provides a possible route to the production of sustainable, high-performance, thermosetting resins with reduced environmental impact.



## INTRODUCTION

Over the last several years there has been a renaissance of activity directed toward the development of full-performance polymeric materials derived from renewable feedstocks.<sup>1–3</sup> These efforts have paralleled similar thrusts in the realm of renewable fuels and chemicals.<sup>4–6</sup> Although the general paradigm is similar in that crude biofeedstocks must first be deconstructed to tractable materials and then chemically converted to molecules with the required properties, the ultimate use of the products dictates the choice of feedstock as well as the methods used to upgrade the biomass. In the case of high temperature polymer systems, the most compelling renewable feedstock is lignin, based on cost, availability, and chemical structure. The long-term cost of crude biomass is estimated at \$60/dry ton, while the U.S. Department of Energy has predicted that up to 1.3 billion tons of biomass (~15–25% lignin) per year could be sustainably produced by 2030.<sup>7</sup> The aromatic structures present in lignin provide excellent high temperature stability combined with low reactivity, flamma-

bility, and hydrophilicity,<sup>8</sup> all important properties for high performance resins. In contrast to other abundant biopolymers, such as cellulose or hemicellulose, lignin is not as attractive for the production of renewable fuels due to its complex structure and recalcitrance. In addition, aromatics do not burn as cleanly as linear or branched chain alkanes and have relatively high melting points. Although methods have been developed to convert lignin to renewable fuels through processes such as pyrolysis, gasification, and hydrolification,<sup>9–11</sup> many of these transformations are hydrogen intensive and are perhaps less practical than other methods. Instead, within the concept of a biorefinery, a compelling case can be made for the production of fuels from the cellulosic and hemicellulosic components of biomass while utilizing the lignin as a source of aromatics, fine chemicals, and polymeric synthons such as phenols.<sup>12</sup> This

Received: November 29, 2012

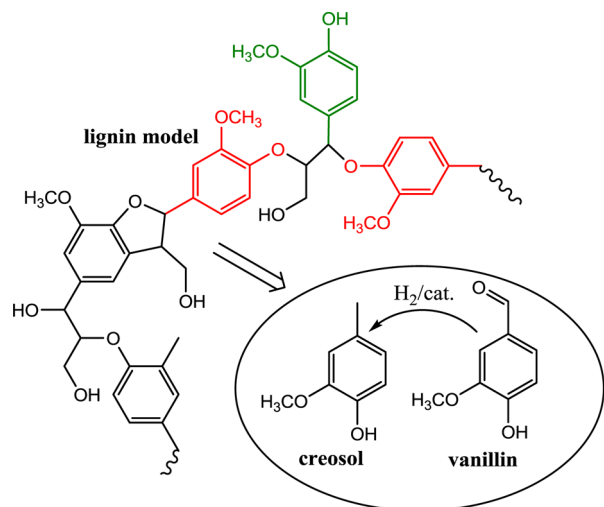
Revised: January 10, 2013

Published: January 16, 2013

parallel approach takes advantage of the chemical diversity of biomass and allows for the production of multiple product streams.

The use of lignin as a significant component of resins and composite formulations has a rich history.<sup>3,9</sup> Lignin has been investigated as a precursor to low-cost carbon fiber,<sup>13</sup> a component of conducting polymers,<sup>14</sup> and a macromonomer useful for the synthesis of polyesters,<sup>15,16</sup> polyurethanes,<sup>17</sup> and epoxy polymers.<sup>18–20</sup> Lignin has also been studied as a replacement for phenol–formaldehyde and urea–formaldehyde resins, sealants, and adhesives.<sup>21</sup> The most straightforward method for incorporating lignin into composites is as an oligomeric species. A disadvantage of this approach is the low degree of functionality per aromatic ring. Although a pure bisphenol has a hydroxyl/aromatic ring ratio of one, the ratio in Kraft lignin is approximately 0.5.<sup>22</sup> This low degree of functionality results in a sparse 3-dimensional network upon cross-linking that is not expected to significantly increase the  $T_g$  beyond that of the native lignin (roughly 150 °C).<sup>23</sup> Although suitable for a variety of commercial applications, this modest glass transition temperature greatly limits the use of lignin in high performance composite materials. In addition, the relatively high melting point of oligomeric lignin reduces the processability of resins and increases the difficulty of composite fabrication. Finally, the complex heteroatom containing structures of the oligomers (Scheme 1) render them susceptible

**Scheme 1. Conversion of Lignin to Well-Defined Phenolics**



to hydrolysis and other cleavage reactions, diminishing the long-term stability of composite materials based on lignin. One way to circumvent these issues is to utilize pure or well-defined mixtures of phenols derived from lignin.<sup>8</sup> Among the candidate phenols, vanillin and 2-methoxy-4-methylphenol (creosol) show a great deal of promise. Oxidation of lignin has been shown to yield up to about 14% vanillin,<sup>24</sup> which has recently been studied as a precursor to both polyvanillin<sup>25</sup> and renewable vinyl esters.<sup>26</sup> Creosol can also be generated from lignin or is readily derived from vanillin through catalytic hydrogenation<sup>27</sup> (Scheme 1).

With the goal of producing renewable precursors to high performance resins, our group recently explored the synthesis of bisphenols from creosol.<sup>28</sup> As a further benefit to its renewable nature, the use of creosol imparts a number of synthetic advantages over simple phenol, including the ability

to selectively generate bisphenols linked through the carbon meta to the hydroxyl group while utilizing stoichiometric amounts of the phenol.<sup>29</sup> Efficient routes to the condensation products of creosol with formaldehyde, acetaldehyde, and propionaldehyde were discovered. In addition, a bisphenol coupled at the position ortho to the phenols was prepared. With the bisphenols in hand it became of interest to synthesize high-temperature cyanate ester resins and to conduct some preliminary experiments to evaluate their suitability for a variety of applications. Cyanate ester resins have been studied extensively over the last several decades<sup>30–32</sup> and more recently by our research group due to a number of advantages over epoxy resins including high glass transition temperatures, low water uptake, and decreased flame, smoke, and toxicity (FST) for both monomers and cured resins. These properties make cyanate ester resins particularly interesting for use in marine and aerospace environments. Recently they have been used or proposed for the fabrication of new high performance components including precision molded nanostructures,<sup>33</sup> magnet casings for thermonuclear fusion reactors,<sup>34</sup> space telescopes,<sup>35</sup> and interplanetary space probes.<sup>36</sup> As an initial entry into the study of renewable cyanate esters, this paper discusses the synthesis, characterization, and cure chemistry of bis(cyanate) esters derived from creosol. These results are discussed within the context of conventional cyanate esters to evaluate both the benefits and limitations of the sustainable materials.

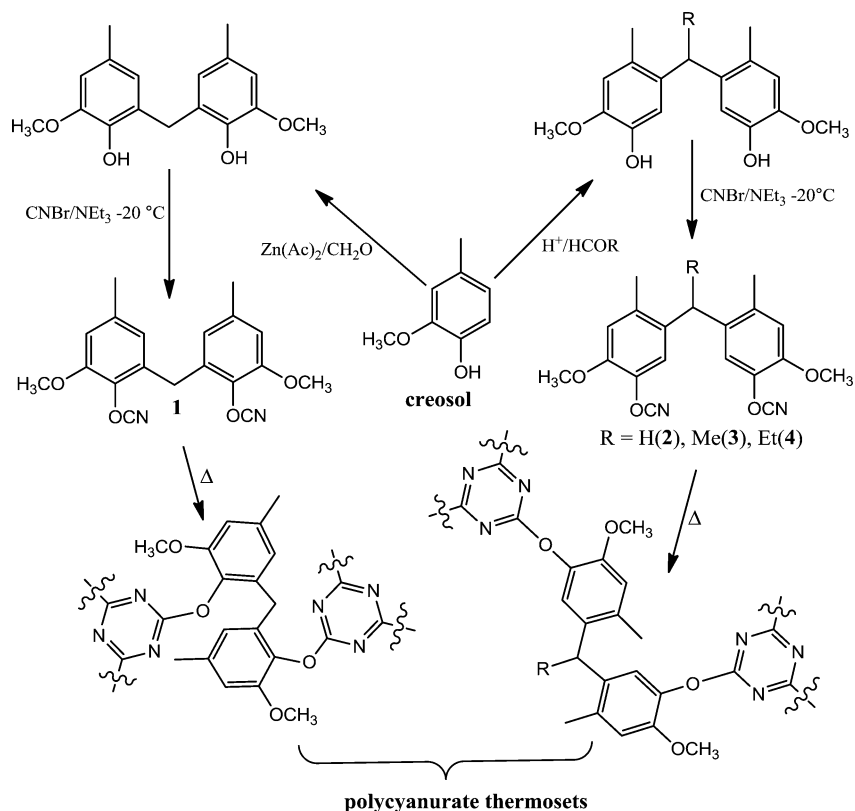
## EXPERIMENTAL SECTION

**General.** The starting bisphenols were prepared as previously outlined.<sup>28</sup> Cyanogen bromide and triethylamine were purchased from Sigma Aldrich and used as received. Anhydrous ether was obtained from Fischer Scientific and used as received. NMR spectra were collected on a Bruker Avance II 300 MHz NMR spectrometer. Samples of the cyanate esters were prepared in  $\text{CDCl}_3$  and spectra were referenced to the solvent peaks ( $\delta = 7.26$  and  $77.16$  ppm for  $^1\text{H}$  and  $^{13}\text{C}$  spectra, respectively). Fourier transform infrared spectroscopy (FT-IR) was carried out using a Thermo Nicolet Nexus 6700 FTIR equipped with the Smart iTr attenuated total internal reflection (ATR) accessory, single bounce diamond crystal. The detector type was a liquid nitrogen cooled MCTA. FTIR spectra are an average of 32 scans, at  $4\text{ cm}^{-1}$  resolution, and have been baseline and background corrected. Melting points were determined with a Mel-Temp apparatus; temperature values are uncorrected. Elemental analysis was performed by Atlantic Microlabs Inc., Norcross, GA.

**General Procedure for Synthesis of Cyanate Esters.** Bisphenol (25 mmol) was dissolved in 100 mL of ether and cooled to  $-78\text{ }^\circ\text{C}$ . Cyanogen bromide (63 mmol) was added to the cooled mixture and allowed to dissolve. Triethylamine (50 mmol) was slowly added dropwise to the cooled mixture over the course of several minutes. The reaction was stirred at  $-78\text{ }^\circ\text{C}$  for 30 min and then slowly warmed up to  $0\text{ }^\circ\text{C}$  and held at that temperature for the duration of the reaction. The reaction progress was monitored by TLC and was complete in  $\sim 3$  h. The products were isolated as outlined below based on the solubility of the final product.

**Bis(2-cyanato-3-methoxy-5-methylphenyl)methane (1).** The reaction mixture was filtered and the residual solid washed with an excess of water to remove  $\text{HNET}_3\text{Br}$ . Yield: 7.62 g (96%) of a white powder. The solid was further purified by dissolving in a minimum of ethyl acetate and then reprecipitating with ether.  $^1\text{H}$  NMR ( $\text{CDCl}_3$ )  $\delta$  2.31 (s, 6H), 3.93 (s, 6H), 4.00 (s, 2H), 6.55 (s, 2H), 6.73 (s, 2H);  $^{13}\text{C}$  NMR ( $\text{CDCl}_3$ )  $\delta$  21.48, 29.67, 56.29, 110.22, 112.64, 122.51, 129.86, 138.67, 138.80, 149.90; mp (powder),  $143\text{--}146\text{ }^\circ\text{C}$ ; (crystals)  $156\text{--}158\text{ }^\circ\text{C}$ ; Elem. Anal. Calcd (%): C, 67.44; H, 5.36; Found: C, 67.17; H, 5.46

Scheme 2. Synthesis of Bis(cyanate) Esters and Polycyanurate Thermosets from Creosol



**Bis(5-cyano-4-methoxy-2-methylphenyl)methane (2).** This compound was isolated in an analogous manner to **1**. Yield: 8.2 g (96% yield) of white solid.  $^1\text{H NMR}$  ( $\text{CDCl}_3$ )  $\delta$  2.25 (s, 6H), 3.78 (s, 2H), 3.92 (s, 6H), 6.82 (s, 2H), 6.86 (s, 2H);  $^{13}\text{C NMR}$  ( $\text{CDCl}_3$ )  $\delta$  19.47, 35.10, 56.30, 109.60, 115.53, 117.51, 130.21, 136.44, 140.28, 146.81; mp 122–124 °C; Elem. Anal. Calcd (%): C, 67.44; H, 5.36; Found: C, 67.50; H, 5.36.

**5,5'-(Ethane-1,1-diyl)bis(1-cyano-2-methoxy-4-methylbenzene) (3).** Volatiles were removed under reduced pressure and the resulting solid was dissolved in ethyl acetate. The organic layer was washed three times with water and dried over  $\text{MgSO}_4$ . Most of the solvent was removed under reduced pressure and then a small amount of ether was added. The mixture was placed at  $-15$  °C to crystallize: 7.93 g (88%) of a white microcrystalline material was obtained.  $^1\text{H NMR}$  ( $\text{CDCl}_3$ )  $\delta$  1.48 (d, 3H,  $J = 7$  Hz), 2.20 (s, 6H), 3.89 (s, 6H), 4.22 (d, 1H,  $J = 7$  Hz), 6.80 (s, 2H), 6.98 (s, 2H);  $^{13}\text{C NMR}$  ( $\text{CDCl}_3$ )  $\delta$  19.15, 20.75, 36.71, 56.25, 109.74, 115.52, 115.69, 135.80, 136.24, 140.34, 146.61; mp 87–88 °C; Elem. Anal. Calcd (%): C, 68.17; H, 5.72; Found: C, 68.24; H, 5.78.

**5,5'-(Propane-1,1-diyl)bis(1-cyano-2-methoxy-4-methylbenzene) (4).** This compound was prepared in an analogous manner to **3**. Yield: 4.25 g (46%).  $^1\text{H NMR}$  ( $\text{CDCl}_3$ )  $\delta$  0.92 (t, 3H,  $J = 7$  Hz), 1.89 (q, 2H,  $J = 7$  Hz), 2.24 (s, 6H), 3.90 (s, 6H), 3.98 (t, 1H,  $J = 7$  Hz), 6.79 (s, 2H), 7.01 (s, 2H);  $^{13}\text{C NMR}$  ( $\text{CDCl}_3$ )  $\delta$  12.56, 19.44, 28.68, 43.66, 56.22, 109.75, 115.63, 115.97, 134.88, 136.28, 140.38, 146.54; mp 115–117 °C; Elem. Anal. Calcd (%): C, 68.84; H, 6.05; Found: C, 68.65; H, 6.02.

**X-ray Diffraction Studies.** X-ray intensity data were collected for omega scans at 296 K on a Bruker SMART APEX II diffractometer with graphite-monochromated  $\text{Mo K}\alpha$  radiation ( $\lambda = 0.71073$  Å). Frames were integrated using the Bruker SAINT software package with a narrow-frame integration algorithm. Data were corrected for absorption using the empirical multiscan method (SADABS), and the structures solved by direct methods using SHELXTL and refined by full-matrix least-squares refinement on  $F^2$ . X-ray data for compounds 2–4 has been deposited in the Cambridge Structural Database.<sup>37</sup>

**TGA/FTIR Analysis.** Samples were analyzed using a Thermo Nicolet Nexus 6700 FTIR interfaced via a heated gas cell and transfer line (held at 150 °C) to a TA Instruments Q50 TGA. The FTIR detector type was a liquid nitrogen cooled MCTA. FTIR spectra are an average of 16 scans, at  $4\text{ cm}^{-1}$  resolution, and have been baseline and background corrected. The TGA was set to ramp from room temperature to 400 °C at a rate of  $10^\circ/\text{min}$ .

**Preparation of Resin Pucks.** Cured polycyanurate samples were prepared by heating the cyanate ester in a 6 mL glass vial to a temperature just above the melting point of the monomer. Once in the liquid state, the material was degassed at 300 mmHg for 30 min and then poured into silicone molds made from R2364A silicone from Silpak Inc. (mixed at 10:1 by weight with R2364B platinum-based curing agent, degassed for 60 min at 25 °C and cured overnight at room temperature, followed by postcure at 150 °C for 1 h and 210 °C for 24 h using a ramp rate of  $5^\circ/\text{min}$  except for **1**, which was cured at 170 °C for 1 h and 210 °C for 24 h. Void-free, transparent, yellow-orange vitreous discs with smooth surfaces and no evidence of shrinkage, bubbles, or phase separation, measuring approximately 11.5–13.5 mm in diameter by 1–3 mm thick and weighing 200–400 mg were obtained by this method. The discs were used for thermomechanical analysis (TMA) and hot water exposure tests.

**Thermoset Characterization.** DSC was performed on a TA Instruments Q200 calorimeter under 50 mL/min of flowing nitrogen. Samples were subjected to a heat-cool-heat cycle from 40 to 350 °C with a ramp rate of  $10^\circ/\text{min}$ . Oscillatory TMA was conducted with a TA Instruments Q400 series analyzer under 50 mL/min of nitrogen flow. The discs were held in place via a 0.2 N initial compressive force with the standard  $\sim 5$  mm diameter flat cylindrical probe, while the probe force was modulated at 0.05 Hz over an amplitude of 0.1 N (with a mean compressive force of 0.1 N). The polycyanurate samples were subjected to two heating cycles and a cycle to determine thermal lag.<sup>38</sup> For samples not exposed to water, samples were cycled twice between  $-50$  and 200 °C at  $50^\circ/\text{min}$  to determine thermal lag with

the exception of **1**, which was cycled between  $-70$  and  $170$  °C. To determine  $T_g$  for **2–4**, the temperature was then ramped to  $300$  °C, cooled to  $100$  °C, and ramped again to  $380$  °C, all at  $50$  °C/min. Compound **1** was ramped to  $250$  °C, cooled to  $100$  °C, and ramped again to  $300$  °C, all at  $50$  °C/min. Discs that were exposed to water were ramped from  $40$  to  $350$  °C, cycled between  $100$  and  $200$  °C to determine thermal lag and ramped again to  $350$  °C, all at  $20$  °C/min. Density of the cured samples was determined using solutions of calcium chloride in deionized water. Discs of the partially cured polycyanurates were placed in a vessel and two solutions, at different concentrations, were combined until a neutrally buoyant solution was obtained. The density of the neutral solution was measured by weighing a  $10$  mL aliquot of the solution using a volumetric flask. This value was compared to the expected density of a calcium chloride solution at the known concentration and ambient conditions. Thermogravimetric analysis (TGA; without FT-IR) was performed on a TA Instruments Q5000 analyzer with either nitrogen or air flow of  $25$  mL/min. The samples were heated from ambient to  $600$  °C at  $10$  °C/min. Moisture uptake experiments were performed using cured discs of uniform  $11.7$  mm diameter and  $3$  mm thickness. Each disk was placed into  $\sim 300$  mL of deionized water maintained at a temperature of  $85$  °C for  $96$  h. The discs were then removed from the water, gently patted dry with a paper towel, and weighed a minimum of three times (all weights agreed to within  $0.0005$  g) and then tested via oscillatory TMA to measure “wet” glass transition temperatures.

**Mass Spectrometry.** Mass spectra of cured resin pucks were obtained by the Direct Insertion Probe method (DIP-MS) using a ThermoFisher DSQII. A small amount of sample was placed in a quartz-micro tube, and inserted into the MS chamber ( $\sim 20$  mTorr) using a direct insertion probe. During analysis the probe was maintained at  $30$  °C for  $30$  s, and the temperature was then increased to  $450$  °C at  $10$  °C/min and held at  $450$  °C for  $5$  min. Mass data were collected for the duration of the temperature program.

## RESULTS AND DISCUSSION

**Synthesis of Bis(cyanate) Esters.** The cyanate esters were readily isolated in good to excellent yields by allowing the bisphenols to react with cyanogen bromide and triethylamine at low temperature (Scheme 2). Diethyl ether was selected as a solvent, and in the case of **1** and **2**, the product cyanate esters precipitated in addition to  $\text{HNEt}_3\text{Br}$ . These solids were readily purified by a water wash followed by recrystallization. In contrast, **3** and **4** with their additional aliphatic carbons maintained a significant amount of solubility in ether, but could be obtained in excellent purity by washing ethyl acetate solutions of the cyanate esters with water followed by crystallization from ether/ethyl acetate solutions. Compounds **1–3** were isolated in nearly quantitative yields, whereas **4**, with its greater solubility in ether, was isolated in  $46\%$  yield.

**Characterization of Bis(cyanate) Esters.** Compounds **1–4** were characterized by  $^1\text{H}$  and  $^{13}\text{C}$  NMR spectroscopy, attenuated total reflectance Fourier transform infrared spectroscopy (ATR-FTIR), elemental analysis, and with the exception of compound **1**, single crystal X-ray diffraction. NMR spectroscopic analysis of compounds **2** and **3** revealed a trace of the cyanate esters with one of the rings bridging through the position ortho to the cyanate ester group. This was predicted based on the starting phenols,<sup>28</sup> but these trace isomers are expected to have only a minor impact on the melting point, cure kinetics, and physical properties of the resins. The IR spectra for **2–4** (Figures S11, S13, and S15) contained two overlapping CN stretching bands due to asymmetric environments for the cyanate ester functionalities in the solid state. In contrast, **1** exhibited only a single broad cyanate ester peak (Figure S9), suggesting that both cyanate

ester groups are in similar environments; this result is in line with the solid state structure of the parent phenol.

The X-ray structures of the cyanate esters (Figure 1) are significantly affected by the aliphatic groups on the bridging

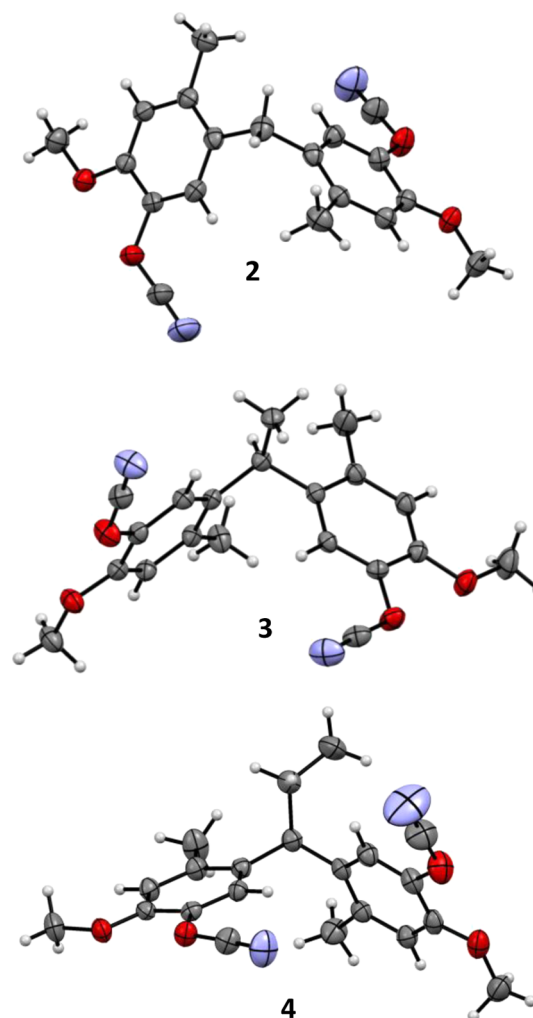


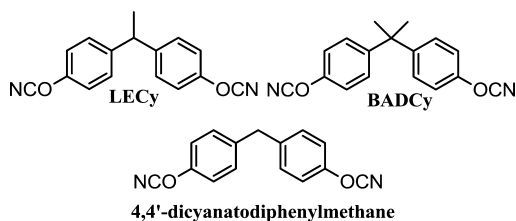
**Figure 1.** Solid state structures of bis(cyanate) esters.

carbon atom. In the case of **2**, the cyanate esters are nearly diametrically opposed with a torsional angle between  $-\text{CN}$  groups of  $157^\circ$ . This configuration also results in an intramolecular  $\text{N–N}$  distance of  $8.292(3)$  Å. In contrast, the methyl group in **3** results in rotation of the aromatic rings and reduces the torsional angle to  $96^\circ$  with an  $\text{N–N}$  distance of  $6.745(3)$  Å. The ethyl group in **4** exerts even more influence on the structure and although the torsional angle ( $97^\circ$ ) is similar to that of **3**, the  $\text{N–N}$  distance is significantly reduced to  $5.139(4)$  Å.

The solid state structures of cyanate esters impart physical properties to the solids that can have important implications for the utility of these materials. Compounds with lower melting points allow for more straightforward fabrication processes that require less energy input. Additionally, for materials that melt at  $<100$  °C, hot water can be used as the heat source to generate molten resins. Although the solid state structures of **3** and **4** are quite similar, the melting points are significantly different with **3** having a melting point almost  $30$  degrees lower than **4** (Table 1). This is similar to the difference in melting point between

**Table 1. Melting Points of Cyanate Esters and Parent Phenols**

| compound | $T_m$ (standard) | $T_m$ (DSC) | phenol $T_m$ |
|----------|------------------|-------------|--------------|
| 1        | 143–146          | 150.7       | 123–125      |
| 2        | 122–124          | 125.4       | 131–134      |
| 3        | 87–88            | 90.8        | 143–146      |
| 4        | 115–117          | 119.6       | Liquid at RT |

**Figure 2.** Structures of conventional cyanate esters.

the conventional cyanate esters LeCy and BADCy (Figure 2), with LeCy existing as a supercooled liquid at room temperature ( $mp = 29\text{ }^\circ\text{C}$ ) and BADCy having a melting point of  $79\text{ }^\circ\text{C}$ . The presence of an unsubstituted methylene linkage, as in 4,4'-dicyanatodiphenylmethane, yields a resin with an even higher melting point ( $108\text{ }^\circ\text{C}$ ).<sup>39</sup>

The melting point trend for the conventional cyanate esters can be explained in terms of a molecular symmetry argument,<sup>40</sup> but for 1–4, such an argument is not complete. Compound 1, which is isolated from a symmetric bisphenol precursor and has been shown to be symmetric in the solid state by IR, has the highest melting point. This is followed by 2, which also has a methylene linkage. Introducing a methyl group at the bridging carbon disrupts the symmetry of the molecule and, as expected, results in a lower melting point. However, introduction of an ethyl group, as in 4, results in a surprising increase in melting point of nearly  $30\text{ }^\circ\text{C}$ . Some insight into this trend can be obtained from a comparison of the space groups of these

cyanate esters (Table 2). Compound 4 crystallizes in the monoclinic  $P121/c1$  space group (Table 2), whereas 3 crystallizes in the triclinic  $P-1$  space group. The higher degree of symmetry inherent to the monoclinic space group provides a possible explanation for the higher melting point of 4. Compound 2 also crystallizes in a monoclinic space group ( $C12/c1$ ), and the similarity between the melting points of 2 and 4 suggests that space group symmetry may be more important for influencing the melting point than the subtle differences between hydrogen, methyl, and ethyl groups on the bridging carbon.

Interestingly, the melting point of the cyanate esters shows the opposite trend compared to the phenols, with the parent phenol of 3 having the highest melting point. However, in the case of the phenols, other effects such as hydrogen bonding play important roles in crystal packing. Also of note, in the case of 1, the cyanate ester has a significantly higher melting point than the parent phenol. Due to the lack of hydrogen bonding in the bis(cyanate) ester, one would expect the opposite result. Unfortunately, we were unable to isolate X-ray quality crystals of 1 that would allow for a comparative study of the solid state structure of 1 with the corresponding phenol.

**Cure Chemistry.** Initial insight into the cure chemistry of these resins was obtained from DSC measurements. Compound 1 melted in the DSC at over  $150\text{ }^\circ\text{C}$  and exhibited a broad and immediate exotherm upon melting that culminated in a peak cure exotherm at  $226\text{ }^\circ\text{C}$ . This lack of a broad processing window or stable temperature range for the molten resin may limit the versatility of this resin for the fabrication of composites. Compound 2, which melted at  $\sim 120\text{ }^\circ\text{C}$ , exhibited a stable processing window but a cure exotherm at the relatively low temperature of  $216\text{ }^\circ\text{C}$ . The enthalpy change for the cure was  $211\text{ kJ}/(\text{mole of compound 2})$  or  $106\text{ kJ}/\text{mol}(\text{cyanate ester})$ , which compares favorably to the widely accepted value of  $100\text{ kJ}/\text{mol}$ . Compound 3 is the lowest melting resin of the four compounds and displays a cure exotherm maximum at  $283$

**Table 2. X-ray Crystallographic Data for Cyanate Esters 2–4**

| property                             | cmpd 2   | cmpd 3   | cmpd 4   |
|--------------------------------------|--|--|--|
| empirical formula                    | $C_{19}H_{18}N_2O_4$   | $C_{20}H_{20}N_2O_4$   | $C_{21}H_{22}N_2O_4$   |
| formula weight                       | 338.35   | 352.38   | 366.41   |
| crystal system                       | monoclinic   | triclinic  | monoclinic   |
| space group                          | $C12/c1$   | $P-1$  | $P121/c1$  |
| unit cell dimensions                 | $a = 17.5687(12)\text{ \AA}$<br>$\alpha = 90^\circ$<br>$b = 4.7770(3)\text{ \AA}$<br>$\beta = 112.4460(10)^\circ$<br>$c = 22.8294(16)\text{ \AA}$<br>$\gamma = 90^\circ$ | $a = 7.062(2)\text{ \AA}$<br>$\alpha = 106.625(4)^\circ$<br>$b = 11.734(4)\text{ \AA}$<br>$\beta = 95.476(4)^\circ$<br>$c = 12.337(4)\text{ \AA}$<br>$\gamma = 105.337(2)^\circ$ | $a = 9.0462(6)\text{ \AA}$<br>$\alpha = 90^\circ$<br>$b = 15.0946(10)\text{ \AA}$<br>$\beta = 102.9660(10)^\circ$<br>$c = 14.9988(10)\text{ \AA}$<br>$\gamma = 90^\circ$ |
| volume                               | $1770.8(2)\text{ \AA}^3$   | $928.4(5)\text{ \AA}^3$  | $1995.8(2)\text{ \AA}^3$   |
| Z                                    | 4  | 2  | 4  |
| density (calcd)                      | $1.269\text{ g}/\text{cm}^3$   | $1.261\text{ g}/\text{cm}^3$   | $1.219\text{ g}/\text{cm}^3$   |
| crystal size (mm)                    | $0.075 \times 0.182 \times 0.212$  | $0.092 \times 0.205 \times 0.433$  | $0.148 \times 0.179 \times 0.340$  |
| $\theta$ (max)                       | $24.99^\circ$  | $25.00^\circ$  | $25.00^\circ$  |
| reflections collected                | 9088   | 10119  | 21371  |
| reflections obsd                     | 953 [ $I > 2\sigma(I)$ ]   | 2291 [ $I > 2\sigma(I)$ ]  | 2693 [ $I > 2\sigma(I)$ ]  |
| independent reflections              | 1563 [ $R(\text{int}) = 0.0430$ ]  | 3281 [ $R(\text{int}) = 0.0245$ ]  | 3504 [ $R(\text{int}) = 0.0253$ ]  |
| data/restraints/parameters           | 1563/0/127   | 3281/0/256   | 3504/0/270   |
| goodness-of-fit on $F^2$             | 1.011  | 1.023  | 1.038  |
| final R indices [ $I > 2\sigma(I)$ ] | $R1 = 0.0415$<br>$wR2 = 0.0917$  | $R1 = 0.0404$<br>$wR2 = 0.0961$  | $R1 = 0.0397$<br>$wR2 = 0.1005$  |

°C with a cure enthalpy of 104 kJ/mol(cyanate ester). Similarly, compound **4** has a cure exotherm maximum at 285 °C and a cure enthalpy of 99 kJ/mol(cyanate ester) (Figure 3). Overall,

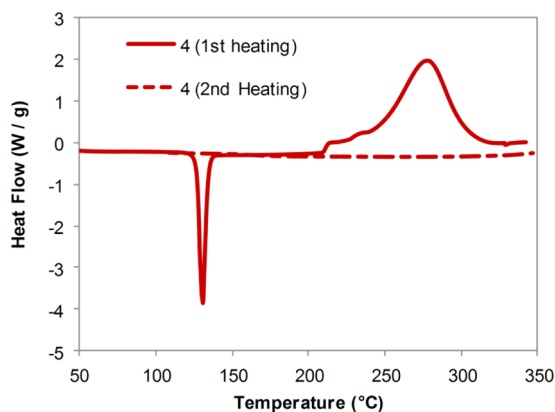


Figure 3. DSC curve for compound **4**.

these data suggest that compounds **2–4** approach complete cure under the DSC conditions. Further evidence of the degree of cure can be extracted from a comparison of the IR spectra of uncured cyanate esters and fully cured thermosets. Figure 4

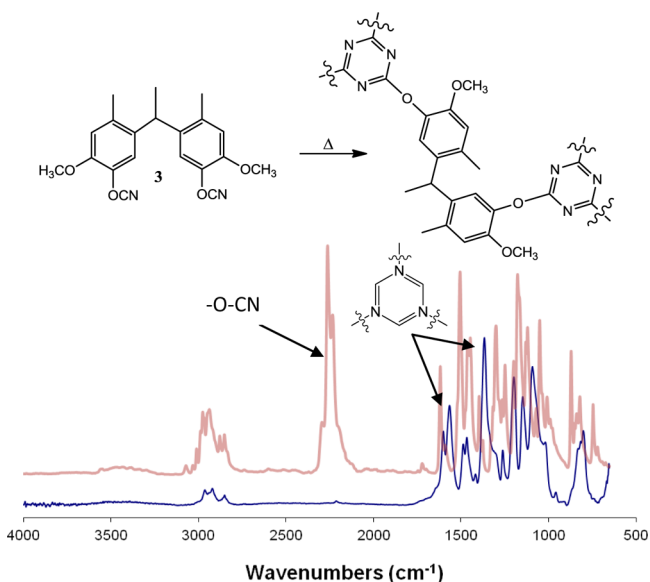


Figure 4. Conversion of compound **3** to a polycyanurate network. The IR spectrum of **3** is shown in red and fully cured resin in blue. Cure conditions: 150 °C, 1 h; 210 °C, 24 h.

shows the results of this comparison for compound **3**, while the data for the other resins can be found in the Supporting Information (Figures S9–S16). These traces show virtually quantitative conversion of the cyanate esters to cyanurate rings for all of the resins. The DSC and infrared spectroscopy results, which are summarized in Table 3, suggest that **3** and **4** are the most promising cyanate esters on the basis of an acceptable processing window and high degree of cure.

To measure the glass transition temperatures of the cured resins, pucks were subjected to TMA analysis. Based on the DSC data it was expected that **1** would not fully cure, leading to a modest glass transition temperature. Indeed this was the case with an as cured  $T_g$  of 181 °C. Further heating to 350 °C

Table 3. Summary of DSC Data for Renewable Cyanate Esters

| compound                    | 1    | 2        | 3        | 4        |
|-----------------------------|------|----------|----------|----------|
| processing window (°C)      |      | ~20      | ~120     | ~60      |
| cure exotherm (max, °C)     | 226  | 216      | 283      | 285      |
| cure enthalpy (kJ/mol, OCN) | 59   | 106      | 104      | 99       |
| degree of cure              | <60% | complete | complete | complete |

actually decreased the  $T_g$  to 178 °C, likely due to decomposition reactions at the elevated temperature. TGA experiments confirmed that **1** experienced significant weight loss at that temperature. The as-cured  $T_g$ s for the *meta*-substituted cyanate esters were all essentially the same at 257 °C, while the fully cured  $T_g$ s ranged from 248 to 214 °C for compounds **2–4**, respectively (Table 4). Again, the cause of

Table 4. Key Properties of Cyanate Ester Resins (High Temperature Cure)

| compound                                 | 1     | 2     | 3     | 4     |
|--|-------|-------|-------|-------|
| density (g/cm <sup>3</sup> )             | 1.237 | 1.223 | 1.198 | 1.190 |
| cyanurate density <sup>a</sup> (mmol/cc) | 2.59  | 2.56  | 2.41  | 2.29  |
| as-cured $T_g$ (LP <sup>b</sup> , °C)    | 172   | 255   | 253   | 254   |
| as-cured $T_g$ (tan $\delta$ , °C)       | 181   | 257   | 257   | 257   |
| fully cured $T_g$ (LP <sup>b</sup> , °C) | 166   | 243   | 196   | 198   |
| fully cured $T_g$ (tan $\delta$ , °C)    | 178   | 248   | 214   | 214   |

<sup>a</sup>For the fully cured samples. <sup>b</sup>LP stands for loss profile.

this decrease in  $T_g$  was attributed to decomposition reactions. Compound **2** is anomalous among these resins, as its  $T_g$  only drops 9° upon heating at the elevated temperature, whereas **3** and **4** both have their  $T_g$  drop 43°. This result is consistent with the observation that pucks formed from **3** and **4** were subject to foaming upon heating to 350 °C. This provided visual evidence that the thermosets had undergone decomposition that resulted in significant outgassing. In contrast, the puck prepared from **2** was intact. The more subtle decrease in  $T_g$  for compound **2** is likely attributable to decomposition reactions on a more modest scale.

In addition to the dry  $T_g$ , it was of interest to evaluate the performance of these thermosets in wet conditions (Table 5).

Table 5. Wet Glass Transition Temperatures and Water Uptake of Resins

| cmpd | wet $T_g$ (tan $\delta$ , °C) | water uptake (%) |
|------|-------------------------------|------------------|
| 1    | 174                           | 2.05             |
| 2    | 193                           | 2.05             |
| 3    | 185                           | 2.61             |
| 4    | 161                           | 3.21             |

To determine a wet  $T_g$ , resin pucks were immersed in 85 °C water for 96 h and then analyzed by TMA. The lowest water uptake was observed for **1** and **2**, while **4** had the highest water uptake. One possible explanation for this behavior is that **3** and **4** cure more completely than **2**. The as-cured  $T_g$  is quite similar for **2–4** even though **3** and **4** would be expected to have lower  $T_g$ s based on their intrinsically more flexible structures. This higher degree of cure then leads to the formation of more void space which increases the uptake of water molecules. Consistent with this hypothesis, the higher uptake of water molecules leads to a greater extent of network hydrolysis, and

thus, lower “wet”  $T_g$  values for 3 and 4. As an explanation for the similarity of the dry and wet  $T_g$ s exhibited by 1, it has previously been observed<sup>38</sup> that cyanurate networks with lower cross-linking densities tend to show “wet”  $T_g$  values very close to the dry  $T_g$  values, apparently because exposure to water results in simultaneous trimerization of unreacted cyanate esters and network hydrolysis.

To minimize any decomposition reactions while allowing the resins to approach complete cure, a new series of pucks were prepared and postcured in the TMA at 250 °C (for 1) and 300 °C for 2–4. These low-temperature conditions resulted in fully cured  $T_g$ s comparable to the as-cured  $T_g$ s while maintaining the integrity of the pucks. In contrast to the high-temperature method, 1 cured completely under these conditions, and all of the resins had similar  $T_g$ s (231–248 °C) with the exception of 3, which had a  $T_g$  of only 219 °C (Table 6). The lower  $T_g$

**Table 6. Glass Transition Temperatures of Cured Resins (Low Temperature Post-Cure)**

| cmpd           | $T_g$ (LP <sup>a</sup> , °C) | $T_g$ (tan $\delta$ , °C) |
|----------------|------------------------------|---------------------------|
| 1              | 236                          | 238                       |
| 2              | 240                          | 248                       |
| 3              | 206                          | 219                       |
| 4              | 219                          | 231                       |
| 4 <sup>b</sup> | 238                          | 244                       |

<sup>a</sup>LP = loss profile. <sup>b</sup>Purified by flash chromatography.

observed for 3 suggests that it does not achieve complete cure under these conditions. Also of interest, the puck made from 4 showed significant degradation and some off-gassing when heated to 350 °C. To determine if this was due to impurities, a sample of 4 was purified by flash chromatography on silica gel and a puck was fabricated. The “high purity” puck had a  $T_g$  13° higher and was stable at 350 °C. This result highlights the fact that the purity of the cyanate esters can have a profound impact on the properties of the resulting thermosets.

To further evaluate the cure chemistry of the cyanate esters, TGA/FTIR data were collected on uncured samples that were heated from ambient temperature up to 400 °C under a nitrogen atmosphere. Gas phase spectra of pyrolysis products were collected with an in-line spectrometer. Compound 1 was stable up to ~350 °C and then rapidly degraded, losing 56% of its mass by 400 °C (Figure 5). In contrast, compounds 2–4 showed significantly different behavior than 1, and these results provided insight into both the cure chemistry and decomposition mechanisms for these resins. Compound 2 exhibited a

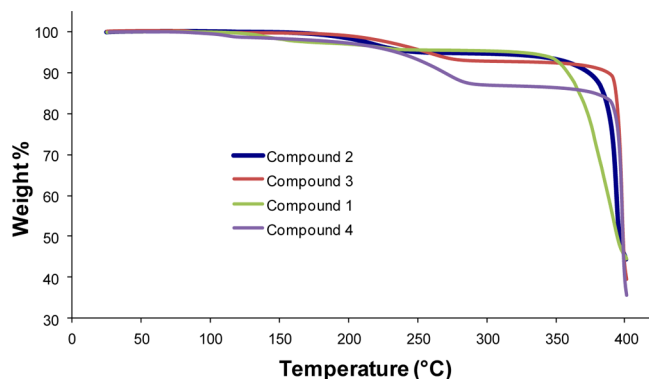
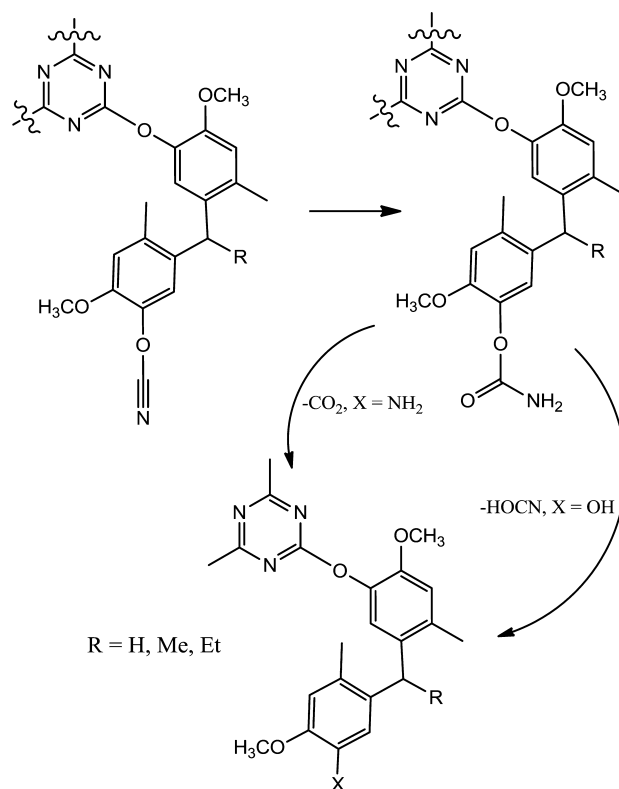


**Figure 5.** TGA (N<sub>2</sub>) of compounds 1–4.

weight loss of about 5% between 180 and 250 °C. After this initial weight loss, the material maintained a consistent weight up to 350 °C followed by an additional weight loss of 7% up to 380 °C and rapid weight loss above this temperature to give 55% weight loss by 400 °C. Compound 3 had a weight loss of 7% between 210 and 280 °C, but unlike 2, compound 3 was stable up to 390 °C and then rapidly degraded. Compound 4 had the highest low temperature weight loss of all the resins (10% between 200 and 290 °C) and then exhibited similar thermal stability to 3 with decomposition occurring at 390 °C.

The gas phase FTIR data of volatile decomposition products collected at low temperature (~200–290 °C) for compounds 2–4 are consistent with evolution of isocyanic acid and suggest that decomposition of a partially reacted polycyanurate network occurs via an unreacted –OCN group that is then converted to a carbamate followed by decomposition to yield a phenol and isocyanic acid (Scheme 3).<sup>41,42</sup> The progressive increase in low

**Scheme 3. Low Temperature Decomposition Pathway for Incompletely Formed Tricyanurate Networks**



temperature weight loss from 2–4 suggests that the molecules with alkyl groups on the bridging carbon atom cure slower than 2. This result is consistent with the greater steric crowding in these molecules, which allows for incomplete networks to exist for longer times at elevated temperatures, resulting in decomposition of unreacted cyanate ester functionalities. Despite this correlation, other factors, particularly the purity of the respective cyanate ester resins, may also play a significant role in the rate of cure. Although all of the resins utilized in this work were shown to be pure by conventional analytical techniques, in other cyanate ester studies, trace impurities (even those around 0.1%) have been shown to have a significant effect on the cure rate.<sup>43</sup> In spite of their propensity to cure slower, compounds 3 and 4 appear to cure more

completely, allowing them to have roughly the same  $T_g$  as **2**, despite the greater flexibility of the native resins. This higher degree of cure also imparts greater thermal stability to the network polymers formed from **3** and **4**, as shown by the delayed onset of high temperature degradation observed from the TGA studies.

For all of the cyanate esters, gas phase FTIR data of the pyrolysis products at 390–400 °C showed evolution of isocyanic acid, methane, and phenolic compounds. The phenols are characterized by a distinctive O–H stretch at 3550  $\text{cm}^{-1}$  as well as two overlapping summation bands at  $\sim 1850 \text{ cm}^{-1}$ . Initially we believed that the primary decomposition products were bisphenols, however, taking compound **3** as an example, comparison of the IR spectrum of the parent bisphenol with the gas phase spectrum of the pyrolysis products (Figure 6) showed

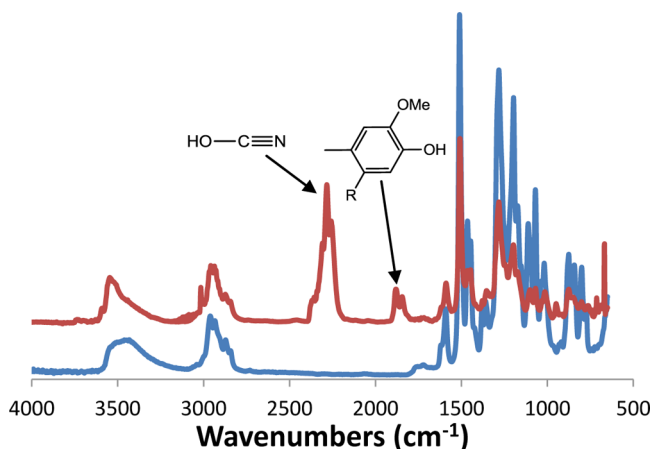


**Figure 6.** Comparison of FTIR data for the phenolic precursor to **3** (blue) and the pyrolysis products observed from the thermoset derived from **3** at 400 °C (red).

that in addition to the bisphenol, the evidence points to cleavage of the bridging group between aromatic rings. Although there is relatively good overlap of the IR bands below  $\sim 1620 \text{ cm}^{-1}$ , the bands at  $1850 \text{ cm}^{-1}$  are particularly diagnostic and match well with the reported spectrum for creosol.<sup>44</sup> To further characterize the decomposition products, we analyzed cured resin samples in a mass spectrometer. Taking compound **3** as an example, the temperature was ramped from ambient temperature up to 450 °C at 10 °C/min. Similar to the IR results, onset of decomposition (under vacuum) was observed at 375 °C and no volatiles were

observed above 440 °C. Although modest peaks were observed for the molecular ion at  $m/z = 302$  and loss of a methylene group at  $m/z = 288$ , the peak with the highest intensity in the mass spectrum had  $m/z = 138$ , which corresponds with creosol. Another significant peak was observed at  $m/z = 152$ , which corresponds to a methyl creosol fragment, ostensibly derived from cleavage of the ethylidene bridging group (Scheme 4). Similarly, the molecular ion peaks of the bisphenols were observed for compounds **1**, **2**, and **4** in their respective spectra, along with cleavage products primarily comprised of alkylated creosols. On the basis of the mass spectrometry results and gas phase IR data, it is clear that the primary decomposition products are the parent phenols along with phenolic fragments generated by cleavage of the aliphatic bridging groups between aromatic rings. The residual cyanurate rings decompose primarily to isocyanic acid.

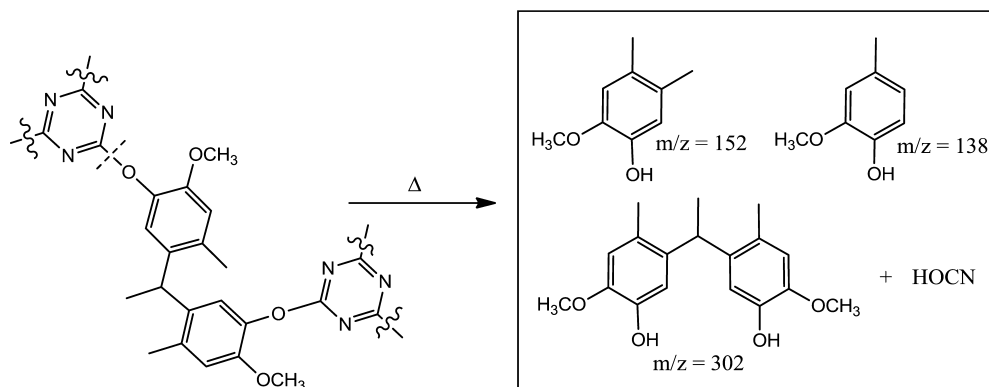
Although these initial TGA/FTIR studies provided insight into both the cure chemistry and the thermal degradation pathways of the materials, these experiments did not allow for an accurate assessment of the stability of fully cured resins. To remedy this, fragments of cured resin pucks were subjected to TGA under both a nitrogen and air atmosphere. In contrast to the TGA results for the uncured samples, no low temperature weight loss was observed due to the presence of a well-formed cyanurate ring network. Interestingly, the weight loss results were similar in both environments up to the decomposition temperature of the resins. In contrast, char yields were significantly lower in air due to oxidation and/or hydrolysis reactions. Although the char yields are somewhat low compared to conventional cyanate esters, this is to be expected due to the lower proportion of aromatic carbons in the renewable resins. Considering loss of all the functional groups except aromatic carbons, a theoretical maximum for char yield is in the range of 39–43% for these resins. The experimental char yield varies from 27 to 35% (Table 7) with **2** producing 81% of the

**Table 7.** TGA Data for Cured Resin Pucks

| compound | $T_{5\% \text{ loss}}$ in $\text{N}_2$ (air), °C | $T_{10\% \text{ loss}}$ in $\text{N}_2$ (air), °C | char yield at 600 °C in $\text{N}_2$ (air), % |
|----------|--|---|---|
| 1        | 317 (326)  | 326 (339)   | 33 (8)  |
| 2        | 360 (357)  | 366 (362)   | 35 (11)                                       |
| 3        | 330 (337)  | 344 (349)   | 28 (11)                                       |
| 4        | 329 (346)  | 345 (357)   | 27 (11)                                       |

theoretical char and **4** producing 69% of the theoretical char. These numbers are in relatively good agreement to BADCY

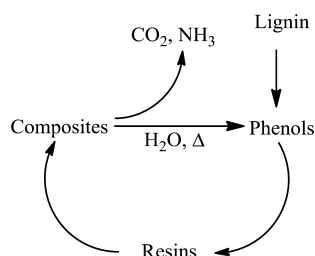
**Scheme 4.** Proposed Decomposition Pathway for the Cured Resin Derived from Compound **3**



(78% of theoretical) but deviate significantly from LECy (94% of theoretical).<sup>45</sup> In the case of 1–4, but also for conventional cyanate esters such as BADCy, some of the loss of char yield is due to evolution of phenolics during decomposition. For 1–4, the char yield in air decreases to roughly 10% at 600 °C for all of the resins, but whether this drop is caused by oxidation chemistry or hydrolysis reactions is unclear.

From a renewable standpoint, the evolution of phenols is quite intriguing and suggests that these resins may potentially be recycled to phenols that could be utilized as precursors to future cyanate esters or a host of other industrial applications. The other main product of the decomposition, isocyanic acid, can be allowed to react with water to produce CO<sub>2</sub> and NH<sub>3</sub>. Although beyond the scope of the current work, one could envision a pyrolytic recycling process (Scheme 5) for out-of-

**Scheme 5. Proposed Recycling Pathway for Renewable Cyanate Ester Resins**



service composite parts fabricated from these cyanate esters. Introduction of stoichiometric water vapor at elevated temperature and under a nitrogen atmosphere would be expected to maximize the formation of phenols, resulting in truly sustainable/renewable materials.

## CONCLUSION

Although the primary focus of this work was to synthesize and evaluate a series of renewable cyanate esters, the results are interesting from other perspectives as well. First, the majority of conventional bisphenols used for the synthesis of epoxy and cyanate ester resins have bridging groups para to the phenol (*p,p*-phenols), whereas phenols with bridging groups meta to the phenol (*m,m*-phenols) are almost nonexistent in the literature. This paper provides some rare insight into the cure behavior of *m,m*-resins. Second, most commercial resins are derived from bisphenols with no heteroatoms, while the resins discussed in this work contain electron donating methoxy groups ortho to the cyanate ester. Despite differences in the cure chemistry and slightly lower thermal stability, the resins described in this paper performed remarkably well considering the structural and electronic differences between these and conventional resins. Third, the potential to recycle thermosetting resins could be of great benefit to society from economical, environmental, and logistical perspectives. Although the current efforts have merely broached the subject, the study of how atypical substituents, such as methoxy groups, affect the decomposition of thermosetting resins could lead to the design of high performance composites that are suitable for use in a variety of applications and environments, but can be easily recycled by thermal and chemical methods.

## ASSOCIATED CONTENT

### Supporting Information

<sup>1</sup>H and <sup>13</sup>C NMR spectra, IR spectra, DSC data, and TGA data for compounds 1–4, a combined .cif file for compounds 2–4, IR spectra, TGA data, and TMA data for the cured resins. This material is available free of charge via the Internet at <http://pubs.acs.org>.

## AUTHOR INFORMATION

### Corresponding Author

\*To whom correspondence should be addressed. Telephone+1 760 939 0247; e-mail [benjamin.g.harvey@navy.mil](mailto:benjamin.g.harvey@navy.mil).

### Notes

The authors declare no competing financial interest.

## ACKNOWLEDGMENTS

The authors would like to thank Ms. Roxanne Quintana for MS analysis and the Strategic Environmental Research and Development Program (SERDP) Project WP-2214 for financial support of this work.

## REFERENCES

- Payne, G. F.; Smith, P. B., Eds. *Renewable and Sustainable Polymers ACS Symposium Series 1063*; American Chemical Society: Washington, DC, 2011; pp 1–212.
- Williams, C. K.; Hillmyer, M. A. *Polym. Rev.* **2008**, *48*, 1–10.
- Stewart, D. *Ind. Crops Prod.* **2008**, *27*, 202–207.
- Climent, M. J.; Corma, A.; Iborra, S. *Green Chem.* **2011**, *13*, 520–540.
- Dinjus, E.; Arnold, U.; Dahmen, N.; Höfer, R.; Wach, W. In *Sustainable Solutions for Modern Economies*; Höfer, R., Ed.; RSC Publishing: Cambridge, 2009; chap. 8, pp 125–163.
- Alonso, D. M.; Bond, J. Q.; Dumesic, J. A. *Green Chem.* **2010**, *12*, 1493–1513.
- U.S. Department of Energy In *U.S. Billion-Ton Update: Biomass Supply for a Bioenergy and Bioproducts Industry*; ORNL/TM-2011/224; Perlack, R.D., Stokes, B.J., Eds.; Oak Ridge National Laboratory: Oak Ridge, TN, 2011; p 227.
- Gandini, A. *Macromolecules* **2008**, *41*, 9491–9504.
- U.S. Department of Energy. In *Top Value-Added Chemicals from Biomass Vol. II: Results of Screening for Potential Candidates from Biorefinery Lignin*; PNNL-16983; Bozell, J. J., Holladay, J. E., Johnson, D., White, J. F., Eds.; Pacific Northwest National Laboratory and the National Renewable Energy Laboratory: Richland, Washington, 2007
- Jae, J.; Tompsett, G. A.; Lin, Y.-C.; Carlson, T. R.; Shen, J.; Zhang, T.; Yang, B.; Wyman, C. E.; Conner, W. C.; Huber, G. W. *Energy Environ. Sci.* **2010**, *3*, 358–365.
- Huber, G. W.; Iborra, S.; Corma, A. *Chem. Rev.* **2006**, *106*, 4044–4098.
- Zakzeski, J.; Buijninx, C. A.; Jongerius, A. L.; Wechhuysen, B. M. *Chem. Rev.* **2010**, *110*, 3552–3599.
- Kadla, J. F.; Kubo, S.; Venditti, R. A.; Gilbert, R. D.; Compere, A. L.; Griffith, W. *Carbon* **2002**, *40*, 2913–2920.
- Kuusela, T. A.; Lindberg, J. J.; Levon, K.; Osterholm, J. E. *ACS Symp. Ser.* **1989**, *397*, 219–227.
- Guo, Z.-X.; Gandini, A. *Eur. Polym. J.* **1991**, *27*, 1177–1180.
- Bonini, C.; D'Auria, M.; Emanuele, L.; Ferri, R.; Pucciariello, R.; Sabia, A. R. *J. Appl. Polym. Sci.* **2005**, *3*, 1451–1456.
- Thring, R. W.; Vanderlaan, M. N.; Griffin, S. L. *Biomass Bioenergy* **1997**, *12*, 125–132.
- Hofmann, K.; Glasser, W. *Macromol. Chem. Phys.* **1994**, *195*, 65–80.
- Ismail, T. N.; Hassan, H. A.; Hirose, S.; Taguchi, Y.; Hatakeyama, T.; Hatakeyama, H. *Polym. Int.* **2010**, *59*, 181–186.
- Nonaka, Y.; Tomita, B.; Hatano, Y. *Holzforchung* **1997**, *51*, 183–187.

- (21) Cetin, N. S.; Ozmen, N. *Int. J. Adhes. Adhes.* **2002**, *22*, 477–480.
- (22) Li, S.; Lundquist, K. *Nord. Pulp Pap. Res. J.* **1994**, *3*, 191–195.
- (23) El Mansouri, N.-E.; Yuan, Q.; Huang, F. *Bioresources* **2011**, *6*, 2647–2662.
- (24) Pandey, M. P.; Kim, C. S. *Chem. Eng. Technol.* **2011**, *34*, 29–41.
- (25) Amarasekara, A. S.; Wiredu, V.; Razzaq, A. *Green Chem.* **2012**, *14*, 2395–2397.
- (26) Stanzione, J. F.; Sadler, J. M.; La Scala, J. J.; Reno, K. H.; Wool, R. P. *Green Chem.* **2012**, *14*, 2346–2352.
- (27) Wang, Q.; Yang, Y.; Li, Y.; Yu, W.; Hou, Z. J. *Tetrahedron* **2006**, *62*, 6107–6112.
- (28) Meylemans, H. A.; Groshens, T. J.; Harvey, B. G. *ChemSusChem* **2012**, *5*, 206–210.
- (29) Conventional phenols, i.e., 3-methylphenol, require high phenol/aldehyde ratios and the reaction is relatively unselective, resulting in multiple products. See, for example, Bogan, L. E.; Wok, S. K. *Macromolecules* **1992**, *25*, 161–165.
- (30) Nair, C. P. R.; Dona, M.; Ninan, K. N. *Adv. Polym. Sci.* **2001**, *155*, 1–99.
- (31) Hamerton, I.; Hay, J. N. *High Perform. Polym.* **1998**, *10*, 163–174.
- (32) Snow, A. W.; Buckley, L. J. In *Handbook of Low and High Dielectric Constant Materials and Their Applications*, Cyanate Ester Resins with Low Dielectric Properties and Applications; Nalwa, H. S., Ed.; Academic Press: San Diego, CA, 1999; pp 189–212.
- (33) Gitsas, A.; Yameen, B.; Lazzara, T. D.; Steinhart, M.; Duran, H.; Knoll, W. *Nano Lett.* **2010**, *10*, 2173–2177.
- (34) Savary, F.; Bonito-Oliva, A.; Gallix, R.; Knaster, J.; Koizumi, N.; Mitchell, N.; Nakajima, H.; Okuno, K.; Sborchia, C. *IEEE Trans. Appl. Supercond.* **2010**, *20*, 381–384.
- (35) Chen, P. C.; Saha, T. T.; Smith, A. M.; Romeo, R. *Opt. Eng.* **1998**, *37*, 666–676.
- (36) Wienhold, P. D.; Persons, D. F. *SAMPE J.* **2003**, *39*, 6–17.
- (37) CCDC 888614 (2), 888615 (3), and 888616 (4) contain the supplementary crystallographic data for this paper. These data can be obtained free of charge from The Cambridge Crystallographic Data Centre through [www.ccdc.cam.ac.uk/data\\_request/cif](http://www.ccdc.cam.ac.uk/data_request/cif). A combined cif file that contains the structural information for each compound is also available in the Supporting Information
- (38) A detailed explanation of thermal lag may be found in Guenther, A. J.; Yandek, G. R.; Mabry, J. M.; Lamison, K. R.; Vij, V.; Davis, M. C.; Cambrea, L. R. Insights into moisture uptake and processability from new cyanate ester monomer and blend studies. *SAMPE International Technical Conference*; SAMPE International Business Office: Salt Lake City, UT, 2010; Vol. 55, p 42ISTC-119.
- (39) Cambrea, L. R.; Davis, M. C.; Groshens, T. J.; Guenther, A. J.; Lamison, K. R.; Mabry, J. M. *J. Polym. Sci. Part A: Polym. Chem.* **2010**, *48*, 4547–4554.
- (40) Brown, R. J. C.; Brown, R. F. C. *J. Chem. Educ.* **2000**, *77*, 724–731.
- (41) Hamerton, I.; Emsley, A. M.; Howlin, B. J.; Klewpatinond, P.; Takeda, S. *Polymer* **2004**, *45*, 2193–2199.
- (42) Kasehagen, L. J.; Haury, I.; Macosko, C. W.; Shimp, D. A. *J. Appl. Polym. Sci.* **1996**, *64*, 107–118.
- (43) Guenther, A. J.; Davis, M. C.; Lamison, K. R.; Yandek, G. R.; Cambrea, L. R.; Groshens, T. J.; Baldwin, L. C.; Mabry, J. M. *Polymer* **2011**, *52*, 3933–3942 and references contained therein.
- (44) IR spectral data can be obtained at the following web address: [http://riodb01.ibase.aist.go.jp/sdbs/cgi-bin/cre\\_index.cgi?lang=eng](http://riodb01.ibase.aist.go.jp/sdbs/cgi-bin/cre_index.cgi?lang=eng)
- (45) Ramirez, M. L.; Walters, R.; Savitski, E. P.; Lyon, R. E. Thermal Decomposition of Cyanate Ester Resins. *DOT/FAA Report AR-01/32*, 2001